Electronic Supplementary Information

Tuning the Surface Reducibility of Perovskite Supports for Optimized Pt-based Alkaline Hydrogen Evolution Reaction Electrocatalysts

Minji Kang[ab†], Won-Gwang Lim[c†], Hoseok Lee[de†], Yeongjun Yoon[f†], Jeseon Lee[g], Juyeon Lee[h], Jaemin Baek[h], Sungjun Kim[a], Tae-Ho Kim[a], Jong Hyeok Park[b], Seonggyu Lee[i], Kyeounghak Kim[f]*, Sung Mook Choi[dj]*, Eunho Lim[gh]**

[a] Hydrogen Energy Research Center, Korea Research Institute of Chemical Technology (KRICT), 141 Gajeong-ro, Yuseong-gu, Daejeon 34114, Republic of Korea

[b] Department of Chemical and Biomolecular Engineering, Yonsei University, 50 Yonsei-ro, Seodaemun-gu, Seoul 03722, Republic of Korea

[c] Chemical and Biomolecular Engineering, Korea Advanced Institute of Science and Technology (KAIST), 291 Daehak-Ro, Yuseong-Gu, Daejeon 34141, Republic of Korea

[d] Energy & Environment Materials Research Division, Korea Institute of Materials Science (KIMS), Changwon 51508, Republic of Korea

[e] School of Energy and Chemical Engineering, Ulsan National Institute of Science and Technology (UNIST), Ulsan 44919, Republic of Korea

[f] Department of Chemical Engineering, Clean-Energy Research Institute, Hanyang University, Seoul 04763, Republic of Korea

[g] Department of Chemical & Biochemical Engineering, Dongguk University, Seoul 04620, Republic of Korea

[h] Department of Energy, Chemical, and Materials Engineering, Dongguk University, Seoul 04620, Republic of Korea

[i] Department of Chemical Engineering, Kumoh National Institute of Technology (KIT), 61 Daehak-ro, Gumi 39177, Gyeongbuk, Republic of Korea

[j] Advanced Materials Engineering, University of Science and Technology (UST), Daejeon 34113, Republic of Korea

† These authors contributed equally to this work

*Corresponding author information
S. Lee: seonggyulee@kumoh.ac.kr
K. Kim: chemekim@hanyang.ac.kr
S. M. Choi: akyzaky@kims.re.kr
E. Lim : eunholim@dgu.ac.kr

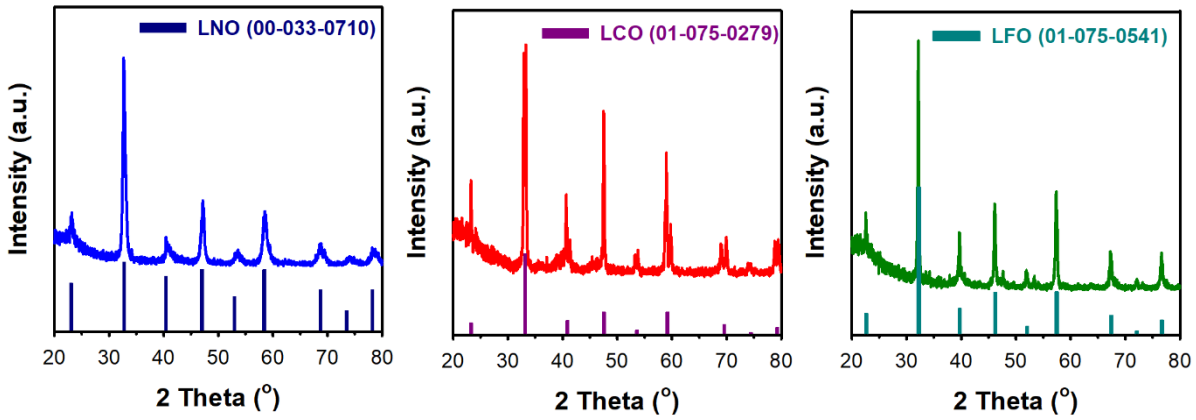

Figure. S1. XRD patterns of LNO, LCO, and LFO measured in the 2θ range of 20−80°.

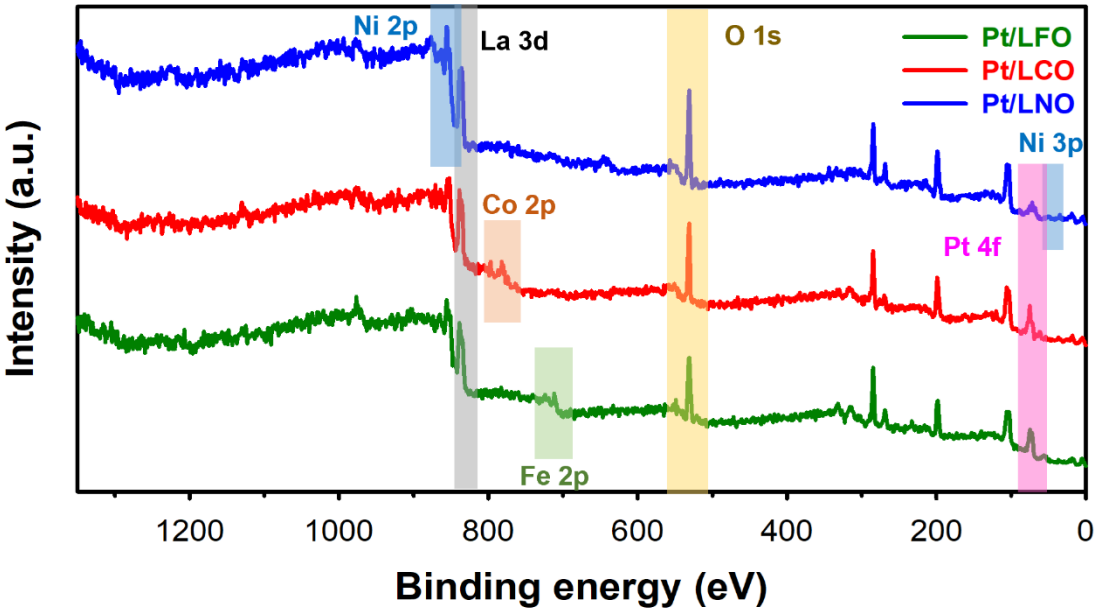

Figure. S2. XPS survey spectra of Pt/LNO, Pt/LCO, and Pt/LFO, demonstrating the surface elemental composition.

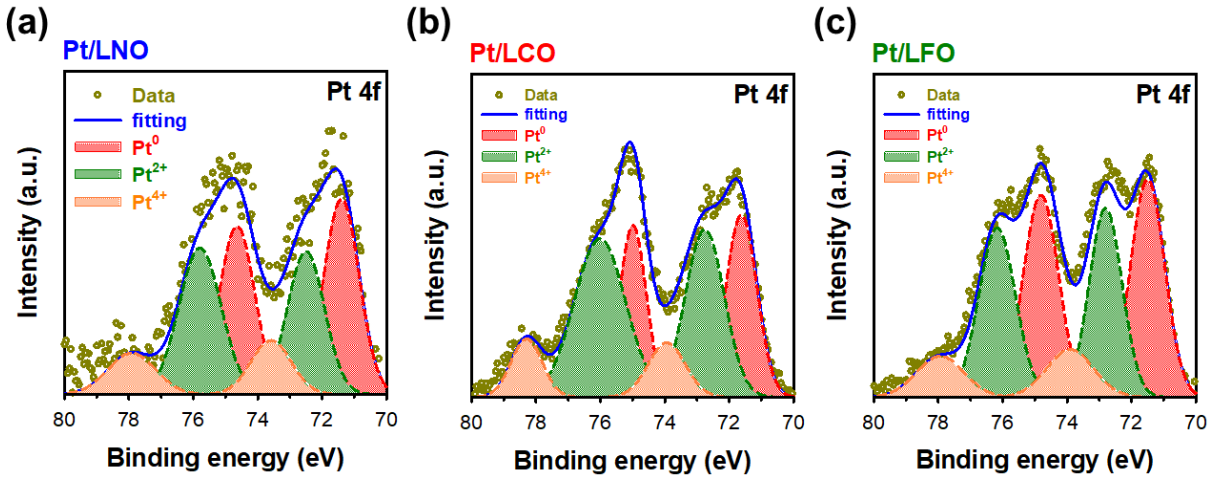

Figure. S3. Pt 4f XPS spectra of (a) Pt/LNO, (b) Pt/LCO, and (c) Pt/LFO, showing the surface chemical states of Pt on each $LaMO_3$ support.

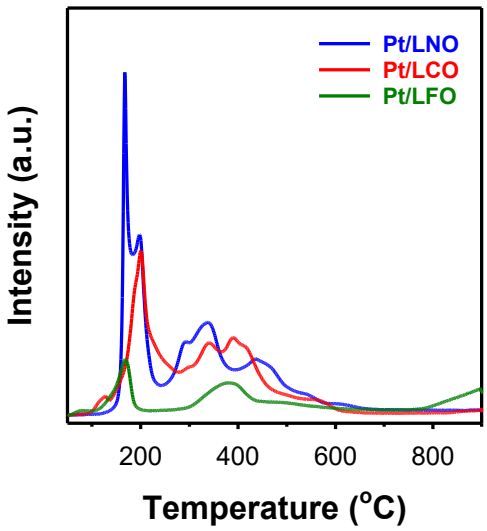

Figure. S4. H_2-TPR spectra of Pt/$LaMO_3$.

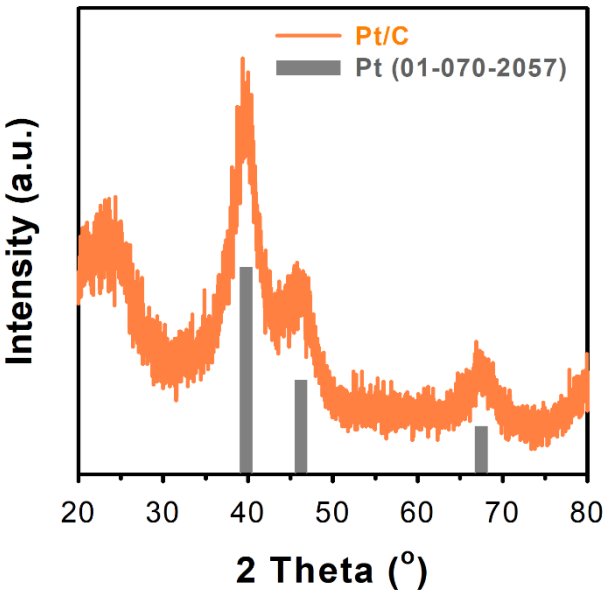

Figure. S5. XRD pattern of the commercial Pt/C (Premetek), measured in the 2θ range of 20−80°.

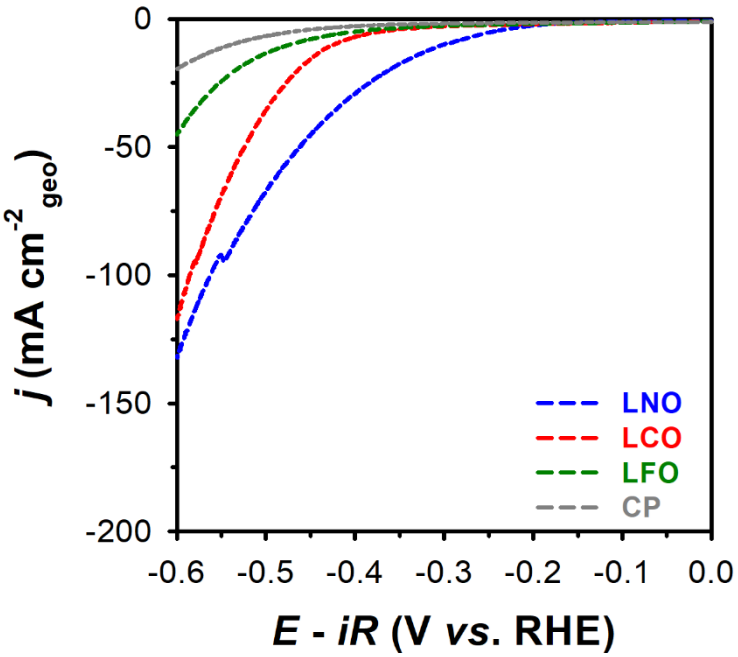

Figure. S6. LSV curves of the pristine $LaMO_3$ perovskite supports and bare carbon paper (CP) measured in a H_2-saturated 1.0 M KOH at a scan rate of 1 mV s^{-1}.

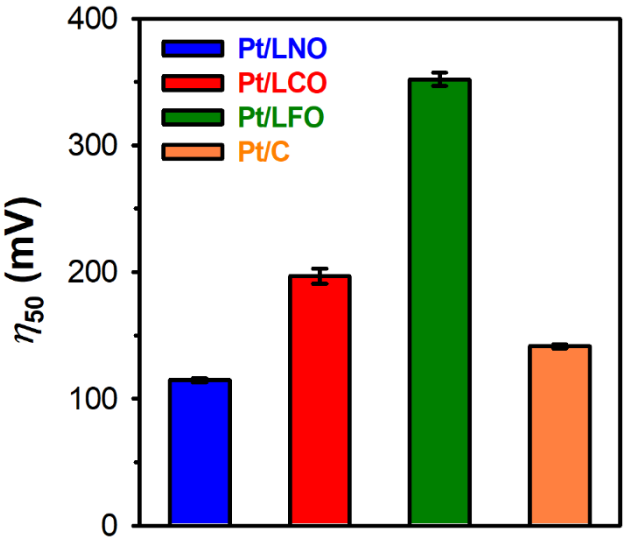

Figure. S7. Summarized η_{50} values of Pt/$LaMO_3$ electrocatalysts and the commercial 20 wt% Pt/C.

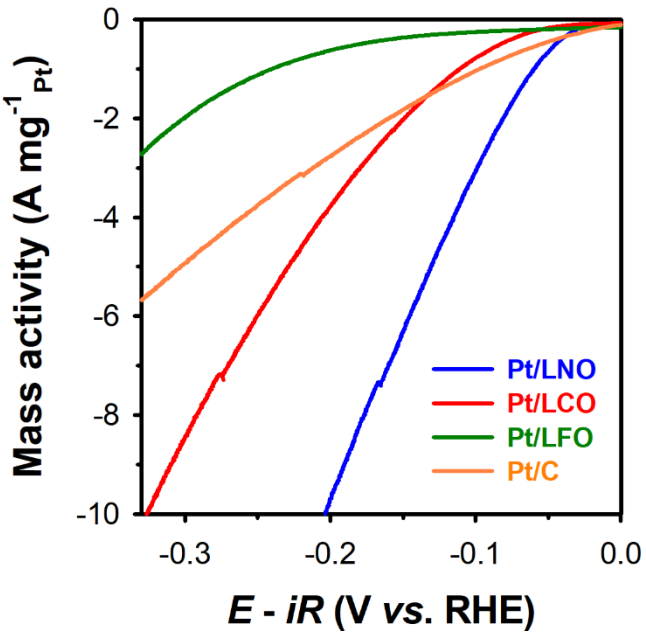

Figure. S8. Mass activity polarization curves of the Pt/$LaMO_3$ electrocatalysts and commercial Pt/C.

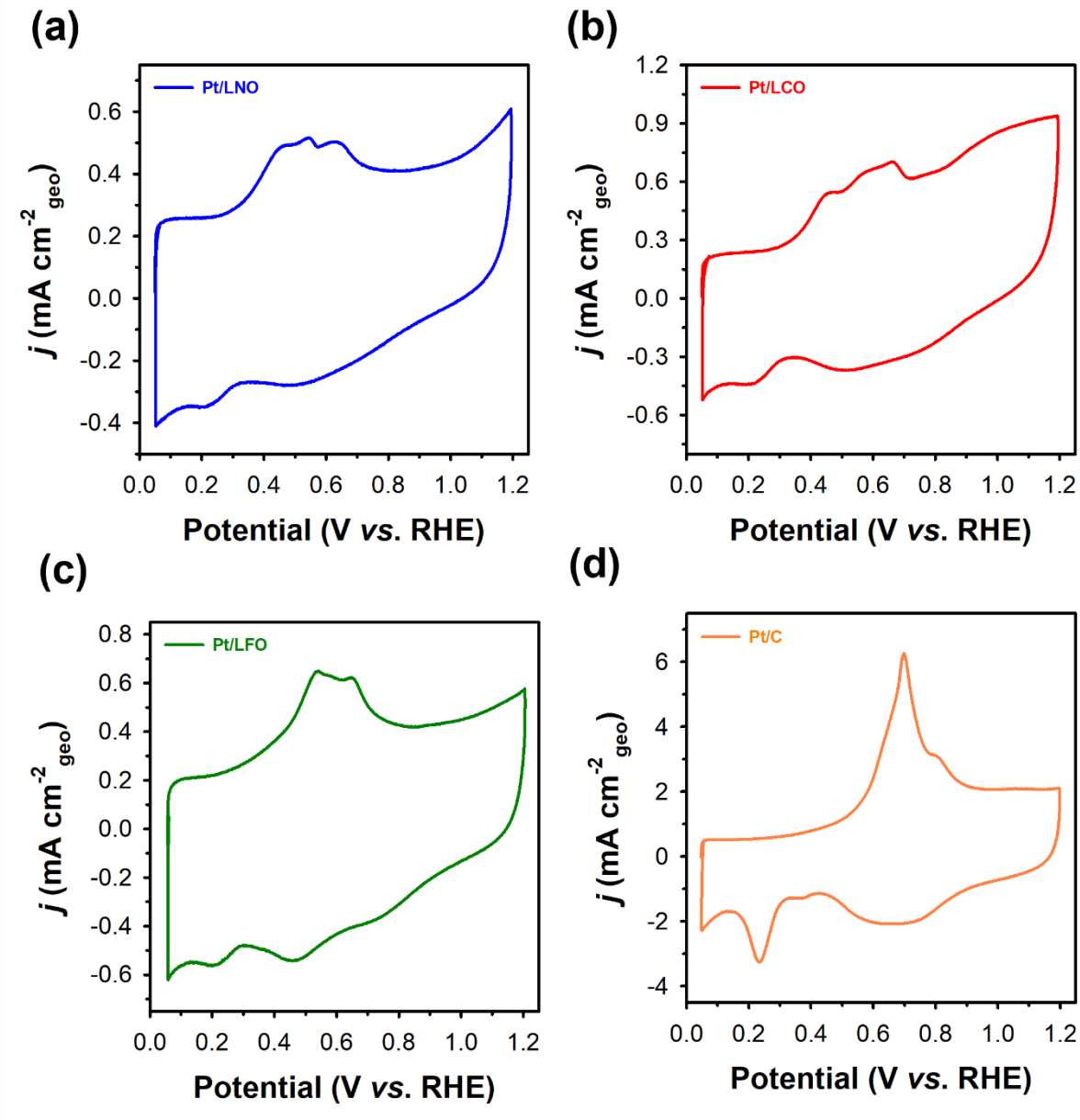

Figure. S9. CV curves based on CO stripping of (a) Pt/LNO, (b) Pt/LCO, (c) Pt/LFO, and (d) Pt/C electrocatalysts, measured at a scan rate of 50 mV s^{-1}.

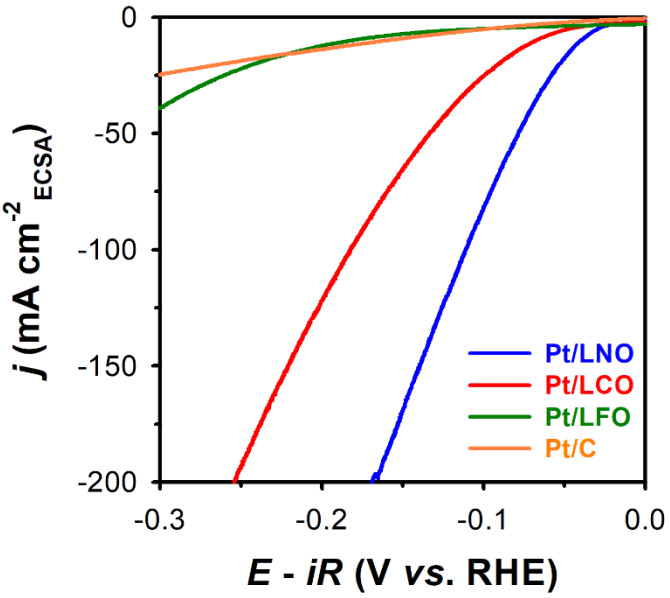

Figure. S10. Specific activity polarization curves of Pt/$LaMO_3$ electrocatalysts compared with commercial Pt/C.

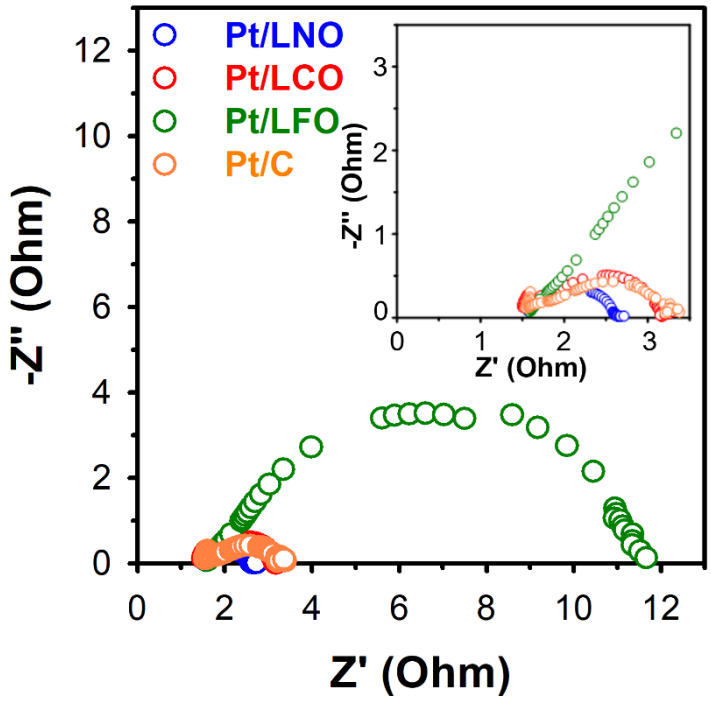

Figure. S11. Nyquist plots of Pt/$LaMO_3$ and Pt/C obtained from EIS measurements conducted at -0.2 V (*vs.* RHE).

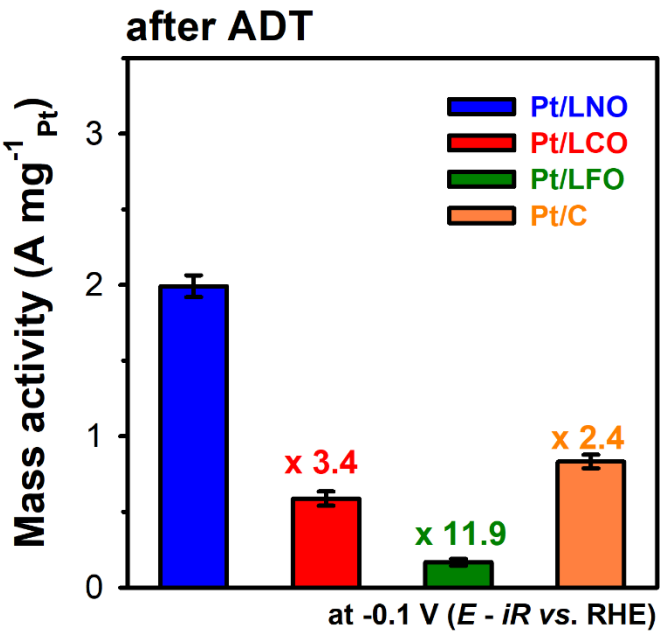

Figure. S12. Post-ADT (Accelerated Durability Test) mass activities of Pt/$LaMO_3$ and commercial Pt/C.

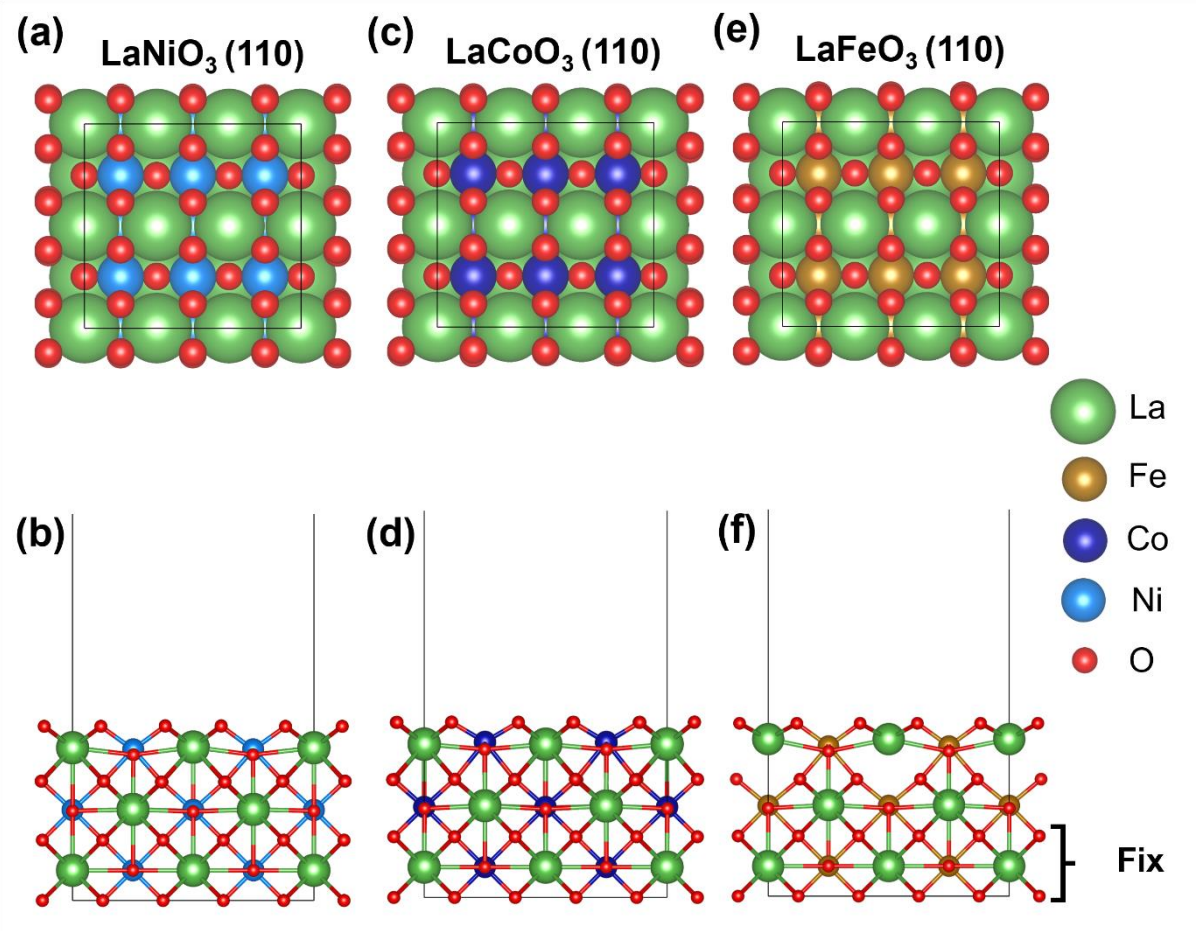

Figure. S13. Top and side views of (a, b) $LaNiO_3$ (110), (c, d) $LaCoO_3$ (110), (e, f) $LaFeO_3$ (110) surface models. The bottom three layers were fixed as the bulk position. The green, brown, blue, gray, and red spheres indicate La, Fe, Co, Ni, and O, respectively.

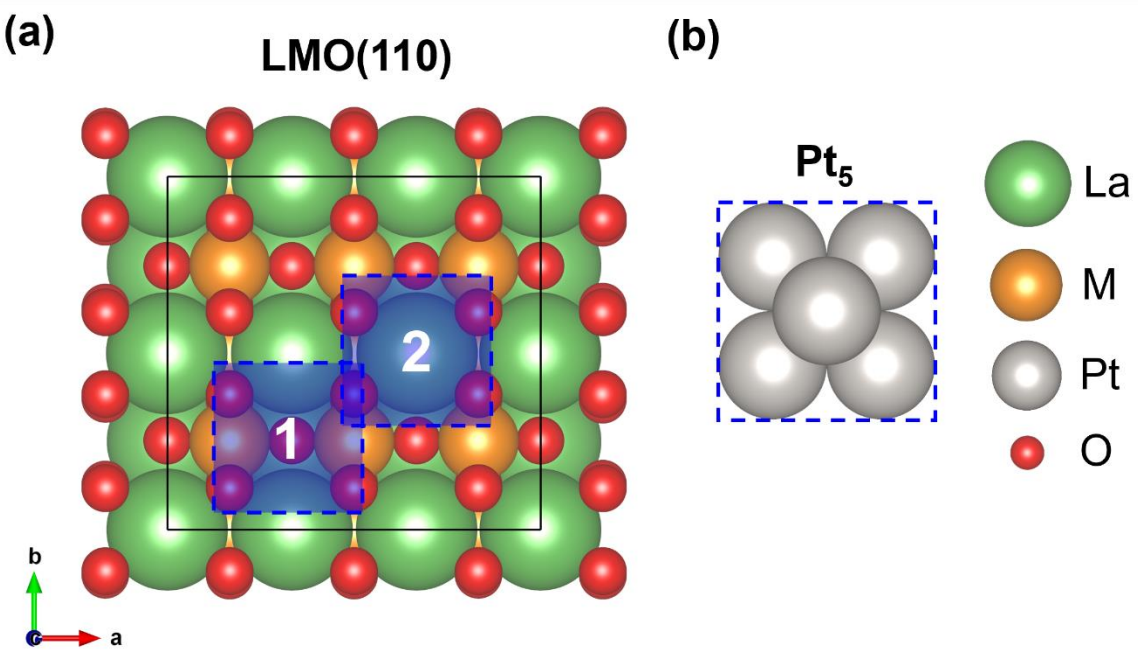

Figure. S14. (a) Top view of $LaMO_3$ (110) (M = Fe, Co, and Ni) surface and two considered positions of Pt_5 cluster (blue-colored area) considering the symmetry of surface atomic arrangement. (b) Top view of Pt_5 cluster.

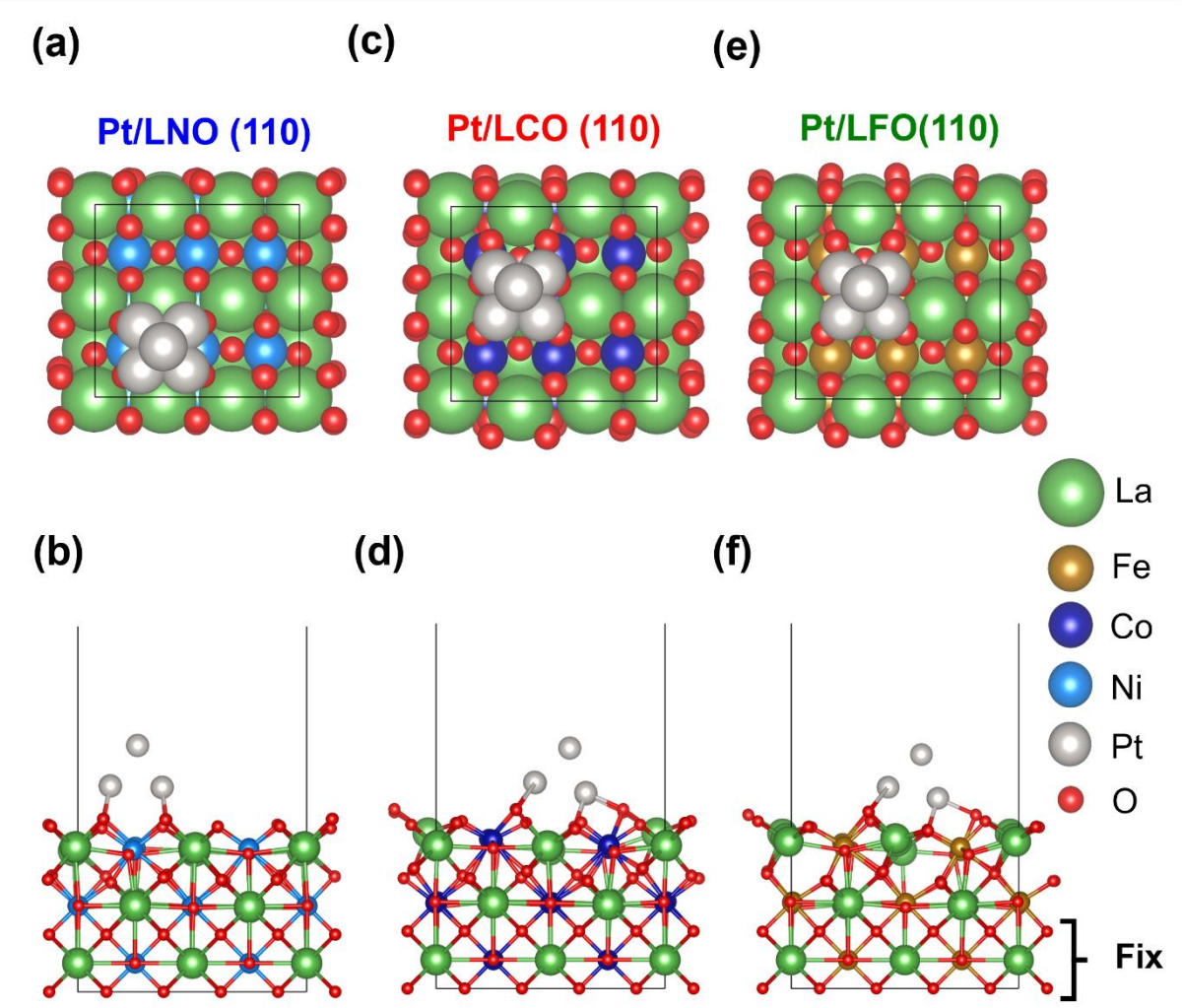

Figure. S15. Top and side views of (a, b) Pt/LNO (110), (c, d) Pt/LCO (110), (e, f) Pt/LFO (110) surface models. The bottom three layers were fixed as the bulk position. The green, brown, blue, cyan, gray, and red spheres indicate La, Fe, Co, Ni, Pt, and O, respectively.

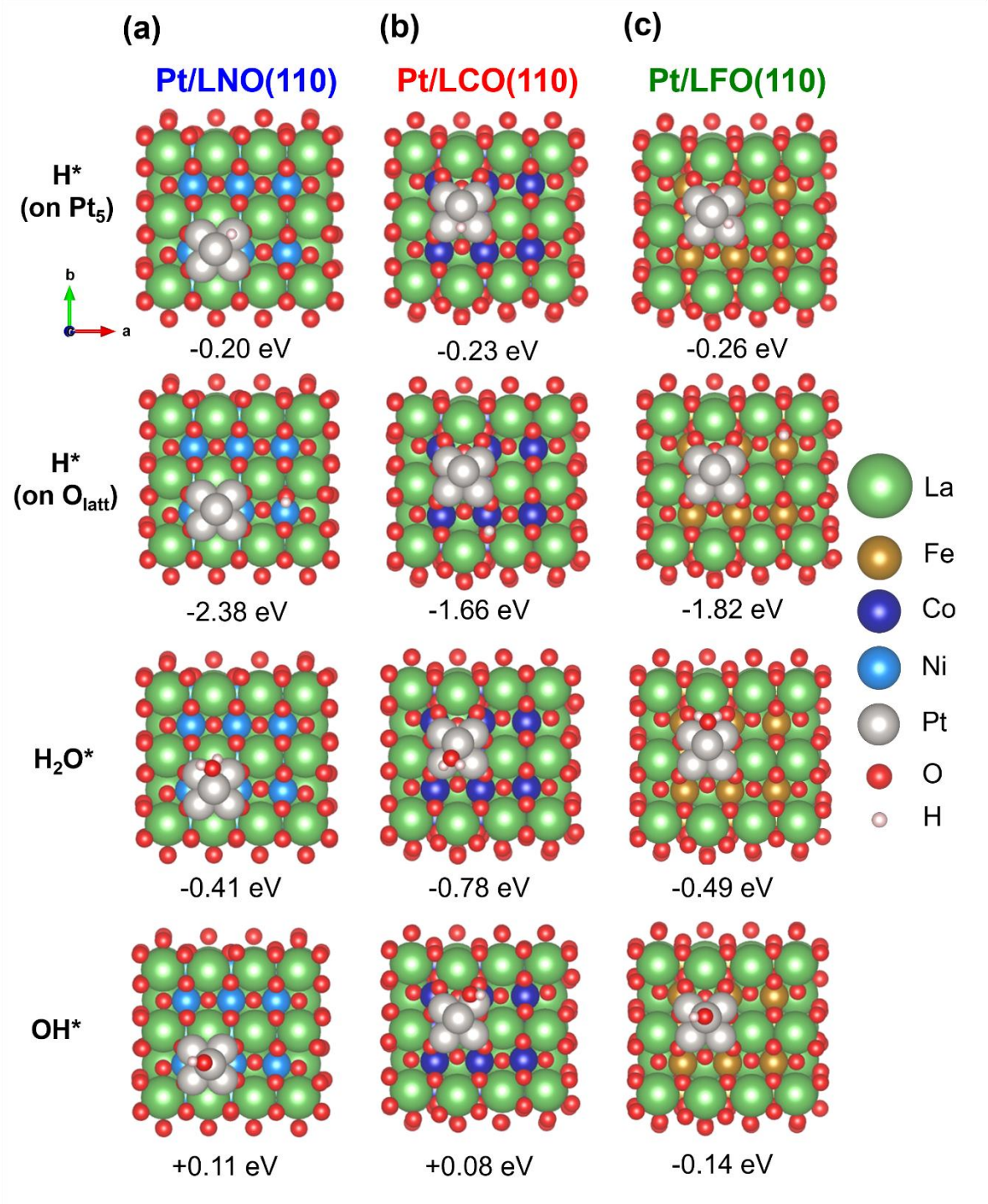

Figure. S16. Top view of the most stable adsorption configuration of H^*, H_2O^*, and OH^* and adsorption free energy corresponding to (a) Pt/LNO (110), (b) Pt/LCO (110), and (c) Pt/LFO (110). The green, brown, blue, cyan, gray, red, and ivory spheres indicate La, Fe, Co, Ni, Pt, O, and H, respectively.

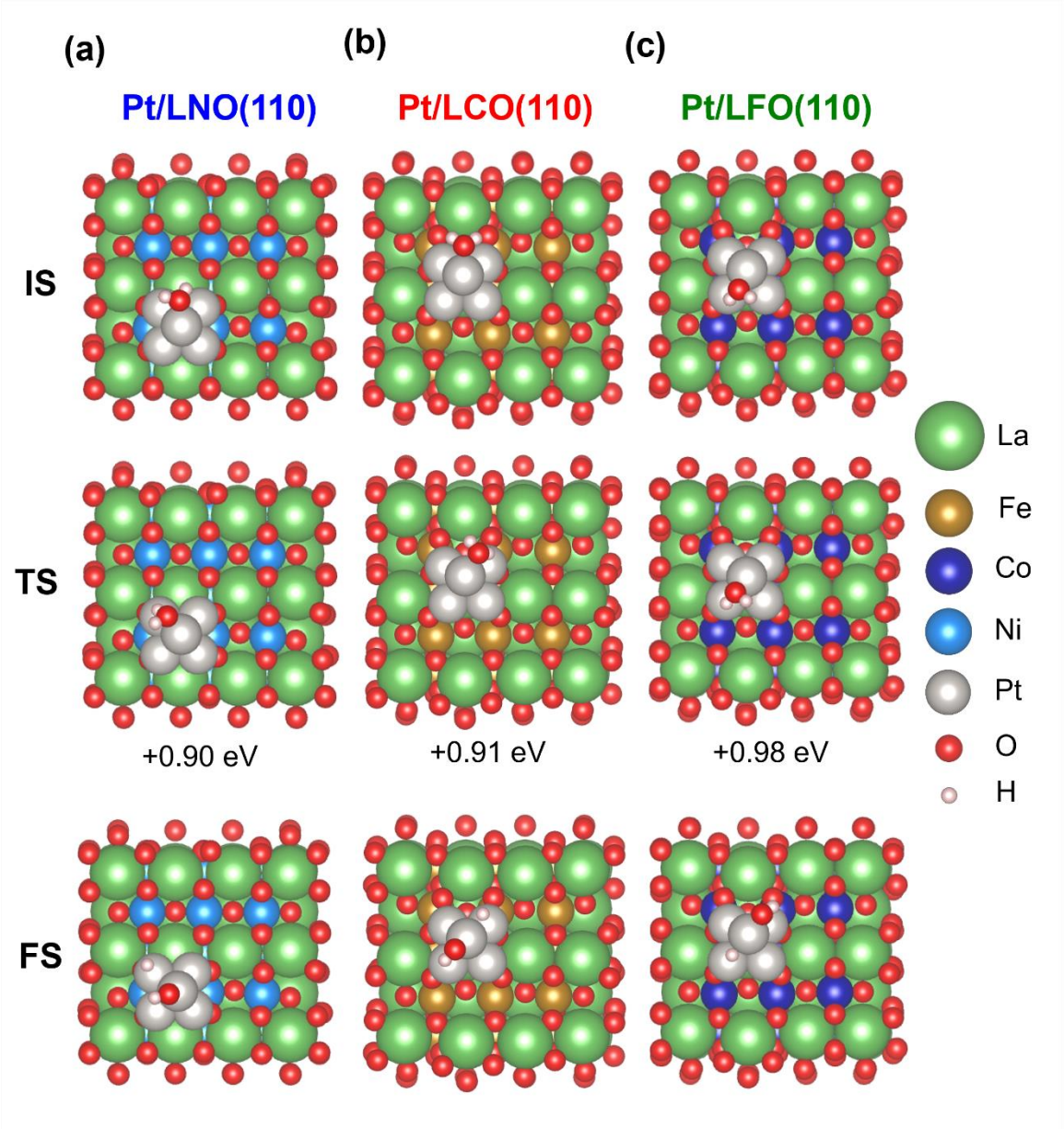

Figure. S17. Initial state (IS), transition state (TS), and final state (FS) of H_2O dissociation reaction on (a) Pt/LNO (110), (b) Pt/LCO (110), and (c) Pt/LFO (110). The green, brown, blue, cyan, gray, red, and ivory spheres indicate La, Fe, Co, Ni, Pt, O, and H, respectively.

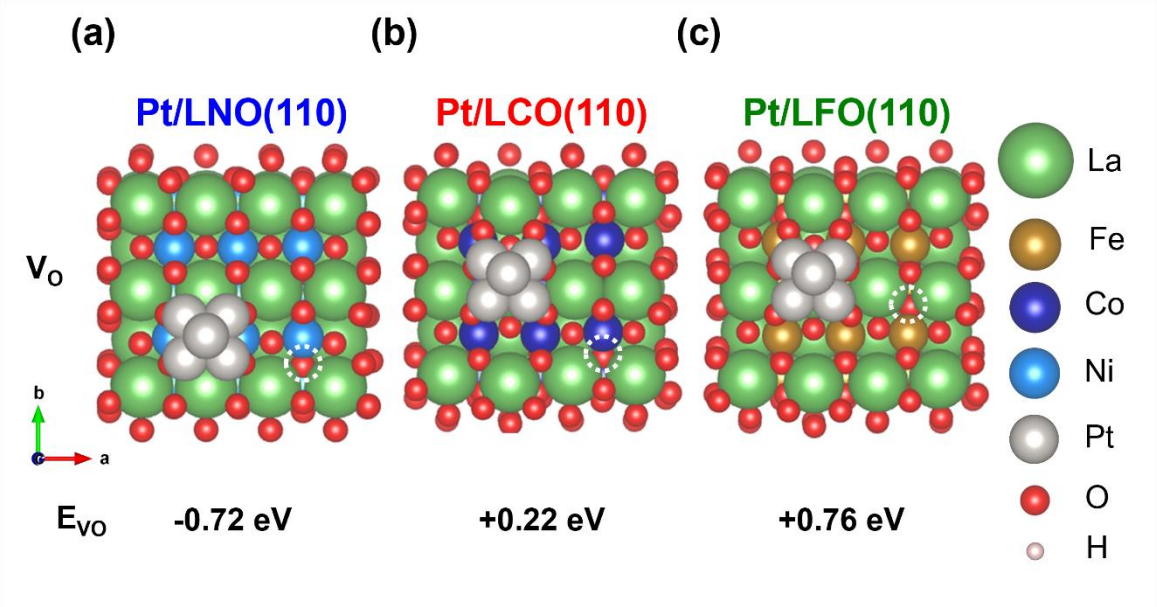

Figure. S18. V_o formation site (white colored dashed line) and oxygen vacancy formation energy (E_{VO}) corresponding to (a) Pt/LNO (110), (b) Pt/LCO (110), and (c) Pt/LFO (110). The green, brown, blue, cyan, gray, red, and ivory spheres indicate La, Fe, Co, Ni, Pt, O, and H, respectively.

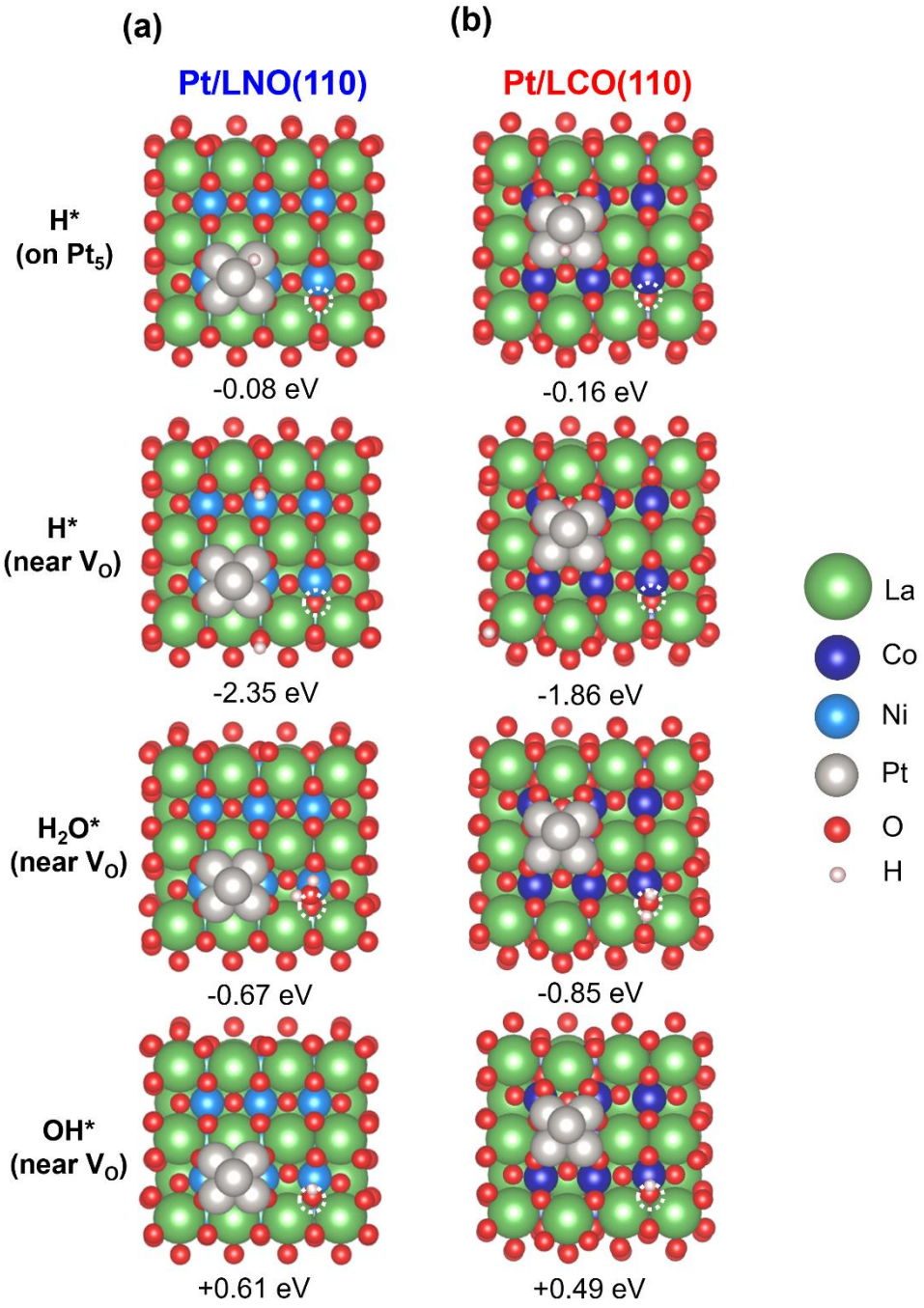

Figure. S19. Top view of adsorption configuration for H^*, H_2O^*, and OH^* adsorption free energies corresponding to (a) Pt/LNO (110) and (b) Pt/LCO (110) with an V_o. White colored dashed line represents the position of V_o. The green, blue, cyan, gray, red, and ivory spheres indicate La, Co, Ni, Pt, O, and H, respectively.

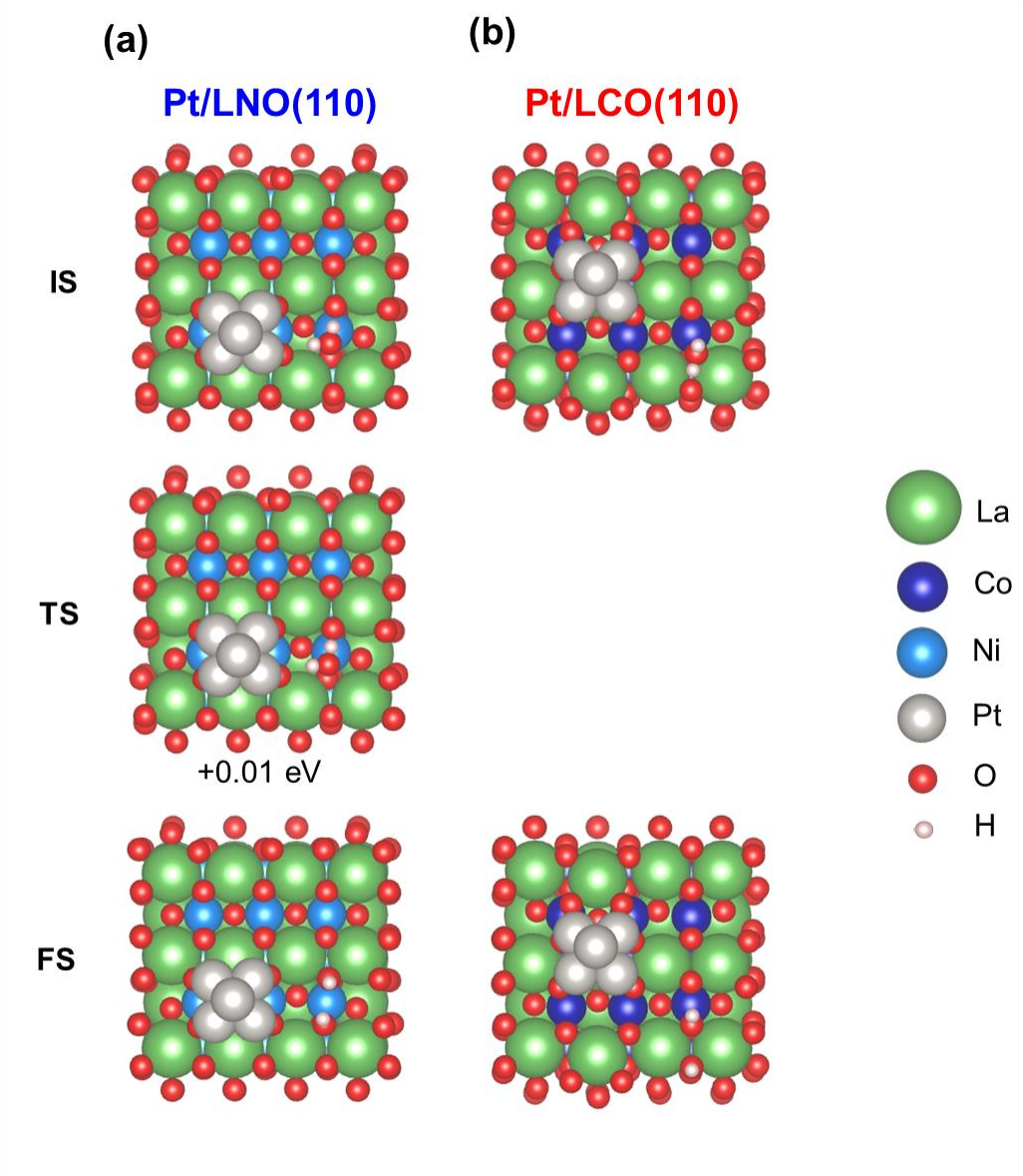

Figure. S20. Initial state (IS), transition state (TS), and final state (FS) of H_2O dissociation reaction on (a) Pt/LNO (110) and (b) Pt/LCO (110) near V_O. The green, blue, cyan, gray, red, and ivory spheres indicate La, Co, Ni, Pt, O, and H, respectively.

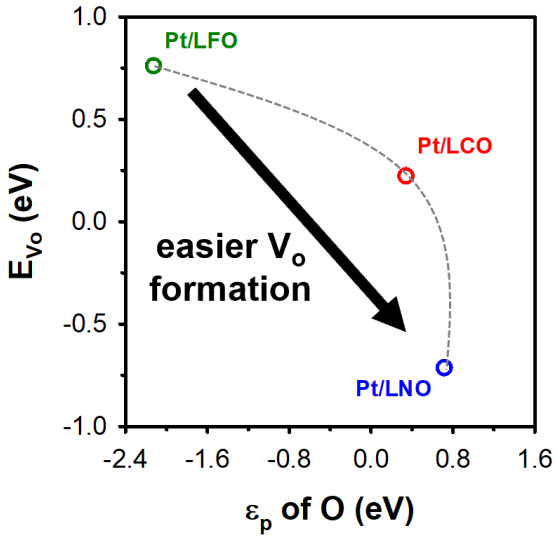

Figure. S21. Correlation between the lattice oxygen *p*-band center, ε_p(O) and E_{Vo} in Pt/$LaMO_3$ (110).

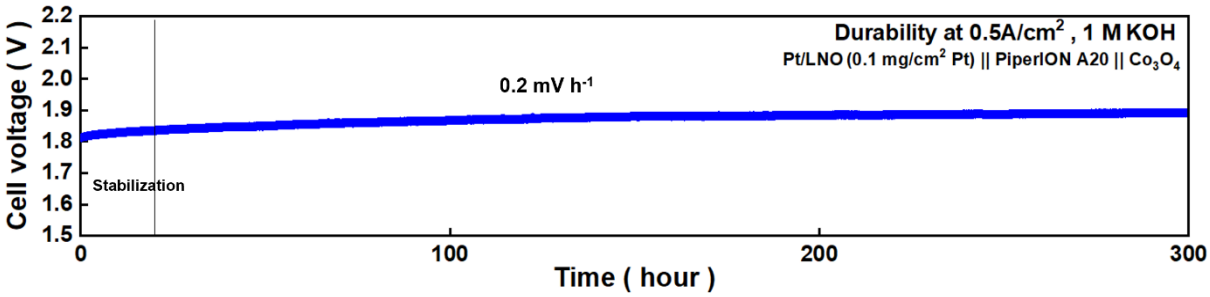

Figure. S22. Long-term stability test of Pt/LNO-based AEMWE with 1.0 M KOH.

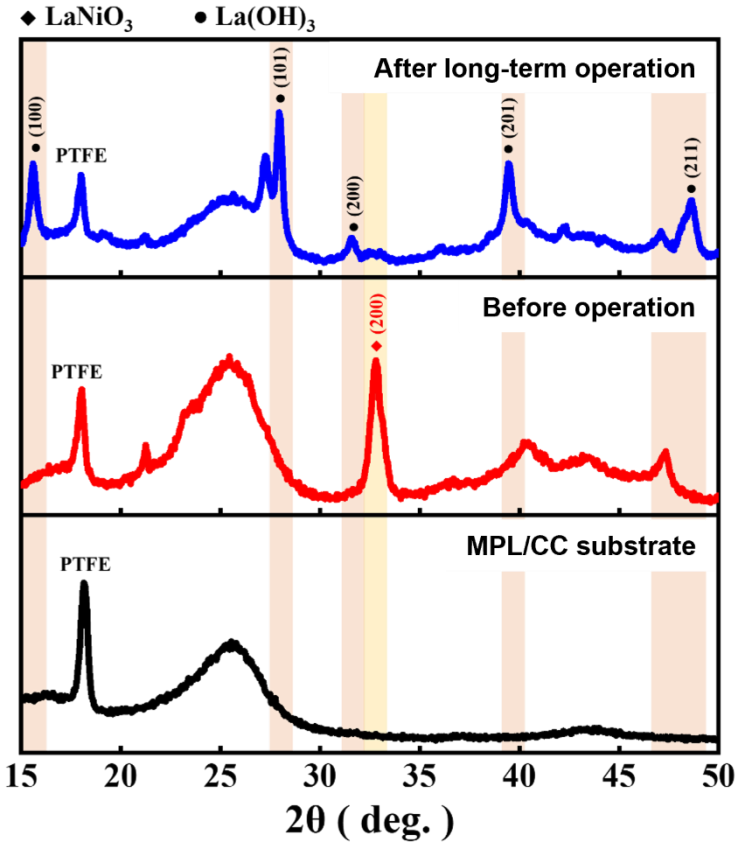

Figure. S23. Ex-situ XRD analysis of Pt/LNO after long-term single cell operation.

Table S1. ICP-OES results showing the measured Pt content in each Pt/$LaMO_3$ electrocatalyst.

Electrocatalyst	Pt (wt%)
Pt/LNO	8.3
Pt/LCO	8.2
Pt/LFO	8.5

Table S2. Summary of the peak area ratios obtained from the O 1s XPS spectra of the Pt/LNO, Pt/LCO, and Pt/LFO electrocatalysts.

Electrocatalyst	O^{2-}	O_2^{2-}/O^-	OH^-/O_2	H_2O
Pt/LNO	3.4%	9.9%	64.6%	22.1%
Pt/LCO	2.4%	8.8%	62.2%	26.6%
Pt/LFO	18.5%	5.4%	50.1%	26.0%

Table S3. Summary of the best-fit parameters from the EXAFS analysis. Parameters marked with an asterisk (*) were fixed during the EXAFS fitting.

Electrocatalyst	Path	Coordination Number	Interatomic distance (Å)	Debye-Waller factor (σ^2/Å^2)	R-factor (%)
Pt foil	Pt-Pt	12*	2.76	0.004	0.002
PtO_2	Pt-O	6*	2.02	0.003	0.013
Pt/LNO	Pt-Cl	1.00	2.22	0.003	0.019
	Pt-Pt	10.13	2.74	0.008	
Pt/LCO	Pt-Cl	1.70	2.29	0.003	0.015
	Pt-Pt	8.88	2.73	0.007	
Pt/LFO	Pt-Cl	0.52	2.22	0.002	0.010
	Pt-Pt	11.48	2.74	0.008	

Table S4. Summary of the calculated ECSA values derived from CO stripping measurements for the electrocatalysts.

Electrocatalyst	ECSA (cm^2)
Pt/LNO	0.4806
Pt/LCO	0.4072
Pt/LFO	0.7348
Pt/C	6.0347

Table S5. Relative total energy (eV) of $Pt_5/LaMO_3$ (110) models with respect to the position of Pt_5 cluster. The green, orange, gray, and red spheres indicate La, M, and O, respectively.

Pt_5 position	Relative total energy (eV)		
	LFO	LCO	LNO
1	+1.70	+1.63	0.00
2	0.00	0.00	+0.03

Table S6. Adsorption free energy (eV) of H^*, H_2O^*, and OH^* on pristine and near V_o on Pt/LFO (110), Pt/LCO (110) and Pt/LNO (110). Gibbs free energy difference (ΔG, in eV) and activation energy (E_a, in eV) at H_2O^* dissociation step. V_o indicates oxygen vacancy.

		Pt/LFO	Pt/LCO	Pt/LNO
H* on Pt_5	Pristine	-0.26	-0.23	-0.20
	Near V_o	-0.17	-0.16	-0.08
H* on oxygen lattice	Pristine	-1.82	-1.66	-2.38
	Near V_o	-1.58	-1.86	-2.35
H_2O^*	Pristine	-0.49	-0.78	-0.41
	Near V_o	-0.56	-0.85	-0.67
OH^*	Pristine	-0.14	+0.08	+0.11
	Near V_o	-0.05	+0.49	+0.61
H_2O^* dissociation (ΔG, E_a)	Pristine	+0.10, +0.91	+0.64, +0.98	+0.32, +0.90
	Near V_o		-0.51, 0.00	-1.07, +0.01